Human Intracranial Atherosclerosis

A Histochemical and Ultrastructural Study of Gross Fatty Streak Lesions

Henry H. Hoff, PhD

A descriptive study of atherosclerotic lesions in human intracranial arteries was undertaken using both light and electron microscopic technics. Arterial segments of human middle cerebral, internal carotid and basilar arteries with gross fatty streak lesions were obtained at autopsy within 4 hours after death, fixed and embedded in plastic. A new technic has been developed in which 0.5 μ-thick sections can be stained with PAS/alcian blue, thereby enabling clear differentiation, substantiated by simultaneous electron microscopic studies, between the lipid-filled smooth muscle cell, which is surrounded by a PAS-positive basement membrane, and the lipid-filled blood monocyte. These technics demonstrated that the gross fatty streak comprised a focal intimal thickening bordered on the lumen by a patent endothelial lining and on the media by a usually intact elastic membrane. The lesion contained smooth muscle cells and cells presumed to be blood monocytes, both filled with and devoid of lipid droplets. Although little fragmented or new elastica was found in the extracellular space, numerous foci of membranous material could be observed, believed to be cell debris and plasma lipoproteins. The similarity between the morphology of such lesions in intracranial arteries with those found in other arterial beds suggests that the documented differences in the prevalence of atherosclerosis in the various beds has no bearing on either the structure of each type of lesion or its progression (Am J Pathol 69:421–438, 1972).

ALTHOUGH MORPHOLOGIC STUDIES of intracranial atherosclerosis using light microscopy have been numerous,[1–7] there are few in which the electron microscope was used.[8–11] To our knowledge no such study has combined histochemical and ultrastructural technics on human intracranial arteries. In a previous communication,[12] I reported the changes in enzyme activity patterns in human intracranial arteries at various stages of atherosclerotic involvement. In the present report, the ultrastructure of the fatty streak lesion from the same material studied previously will be described. Furthermore, a modification of the PAS/alcian blue stain was employed on semithick sections of plastic-embedded material to obtain high resolution light micro-

From the Department of Neurology, Baylor College of Medicine, Houston, Tex.

Supported in part by Grants NS-09287 and HE 13669 from the National Institutes of Health.

Accepted for publication Aug 3, 1972.

Address reprint requests to Dr. Henry H. Hoff, Department of Neurology, Baylor College of Medicine, 1200 Moursund Ave, Houston, Tex 77025.

scopy survey pictures of atherosclerotic lesions. Such combined morphologic approaches to atherosclerotic lesions may eventually help elucidate reasons for the variation in incidence of the disease process for each age group in intracranial and other arterial beds.[13]

Materials and Methods

Human middle cerebral, internal carotid and basilar arteries were obtained, at autopsy, within 4 hours after death; findings have been reported elsewhere.[12] The subjects' ages ranged from 37 to 78 years. Segments of arteries were prefixed in 2.5% paraformaldehyde–2.5% glutaraldehyde in 0.1 M cacodylate buffer, pH 7.4; washed in the cacodylate bucer overnight and postfixed in 1% osmium tetroxide in 0.1 M cacodylate buffer, pH 7.4, for 2 hours at 4C; dehydrated in graded ethanols and embedded in Epon. Semithick (0.5 μ) and ultrathin sections were cut on a Reichert UM2 Ultramicrotome. Semithick sections were stained with 1% alkaline toluidine blue and by a modified PAS–alcian blue procedure after the plastic was extracted with a saturated sodium hydroxide solution in absolute ethanol, using a modification of the procedure described by Mayor *et al.*[14] Ultrathin sections were doubly stained with aqueous uranyl acetate and lead citrate, and viewed with an RCA UM4 electron microscope.

Results

Light Microscopic Observations

Semithick sections of atherosclerotic intracranial arteries were stained with PAS–alcian blue. In black and white photography (Figures 1 and 2), the red PAS-positive material appeared quite dense when a green filter was used. Smooth muscle cell contours are seen particularly well, since their PAS-positive basement membranes are well delineated. Although alcian blue-positive material was poorly discerned under these conditions, this stain functions as a nuclear counterstain even better than hematoxylin, which was found to overshadow the red PAS-positive stain.

A number of generalizations may be made from the data obtained by viewing the semithick sections at low power. Gross fatty streak lesions are comprised of focal areas of intimal thickening, which are most often eccentric and thinner in the smaller middle cerebrals, while they were frequently concentric and up to 20 cell layers thick in the larger internal carotid and basilar arteries. Otherwise, the lesions were identical in all large intracranial arteries. In such lesions most of the cells had a fusiform shape and did not show consistent orientation. Lipid droplets, although rare in endothelial cells, were numerous in both fusiform and round cells. Ultrastructurally, these latter cells were shown to be smooth muscle and foam cells, respectively. Most of the lipid droplets in foam cells were seen as round vacuoles of a uniform

size (Figures 7A and B). Areas were found in fatty streak lesions in which lipid droplets were confined to either foam or smooth muscle cells (Figures 2A and D). However, in most cases, fat vacuoles were found in both cell types (Figures 1F and 2F). The localization of foam cells in the intima varied from areas just subjacent to the endothelium to areas deeper in the intima. Numerous PAS-positive granules were found interspersed between lipid droplets in foam cells (Figures 2D to 2H). PAS-positive basement membrane circumscribed only the smooth muscle cells. Frequently, the material appeared fragmented or even absent around portions of cells (Figures 2C and 2H). The intensity and thickness of the PAS stain was greater around medial than around intimal smooth muscle cells (Figure 1G). A thick band of PAS-positive material was often found just subjacent to the endothelium (Figure 2A), while both the elastica and the narrow areas between foam cells had a pink hue (Figures 2A, B and H). Elastica fragmentation or reduplication was rarely seen in such fatty streak lesions.

Electron Microscopic Observations

The fatty streak lesion was comprised of four morphologically distinguishable types of cells: a) the endothelium, which appeared unaltered from its morphology in uninvolved segments (Figures 3A and 4A); b) the smooth muscle cell; c) the round foam cell; and d) a mononuclear cell devoid of lipid droplets (Figure 3B).

The foam cells contained uniform lipid droplets, ranging in morphology from empty vacuoles, both with and without limiting membranes, to vacuoles with partially extracted centers (Figures 5 and 6). Certain cells contained a multitude of vacuoles filled with electron-dense membranous structures (Figure 7A). These cells were usually adjacent to an area of extracellular debris which closely resembled the contents of the foam cell vacuoles (Figure 7A). Microfilaments, clusters of ribosomes, smooth and rough endoplasmic reticulum, Golgi zones and numerous dense bodies, containing crystalline and whorl bodies, were observed in foam cells (Figures 5 and 6). Numerous finger-like processes extended from the foam cells, forming tightly interdigitating junctions when two or more foam cells were grouped together (Figure 5A). Gaps between foam cells were often quite straight (Figure 5B).

The mononuclear cell, seen often in close apposition to foam cells (Figures 3B and 7B), resembled the latter in most respects, except in containing lipid vacuoles. Somewhat unique were the long strands of what appears to be rough-surfaced endoplasmic reticulum (Figure

7B). As in foam cells, these cells lacking cell membrane invaginations had free ribosomes, round mitochondria and numerous foot processes which formed interdigitating junctions with foam cells.

The smooth muscle cell of the fatty streak lesion resembled its counterpart in the media. It was smaller, however, and its basement membrane was often either fragmented or, focally, not present. This cell often contain lipid droplets nonuniform in size but of uniform density and lacking a limiting membrane (Figures 3A and 4); a contrast to the foam cell in which most of the cytoplasm was filled with lipid droplets that appeared to have a tendency to coalesce (Figure 4). On rare occasions, smooth muscle cells also contained crystalline material (Figure 3A). Frequently, cytoplasmic extensions were seen intermingled between foam and smooth muscle cells (Figure 7B).

The extracellular space often contained electron-dense membranous structures (Figure 7A). Focal areas of necrosis were completely filled with such structures as well as with crystalline material. Round and reticulated electron-translucent material, adjacent to the flocculent and granular-basement membrane and to the elastica, was abundant between smooth muscle cells (Figure 4). Especially in the smaller middle cerebral arteries, the thick basement membrane under the endothelium was widened and fragmented.

Discussion

The gross fatty streak lesion in human intracranial arteries has been extensively described. In the ensuing discussion, the similarities of numerous morphologic alterations between such lesions and those in other arterial beds, both in humans and experimental animals, will be reviewed.

The focal nature of the intimal elevations comprising the fatty streak lesion has been documented in sheep cerebral arteries.[6] Focal accumulation of intra- and extracellular lipid in the arterial intima, except for areas in which the elastica was fenestrated or fragmented, has been cited in light microscopy studies of cerebral arteries, both in humans [1,5,7] and in swine.[9] The further widening and fragmentation of the thick basement membrane-like and PAS-positive material subjacent to the endothelium was reported in middle cerebral arteries of humans,[8] swine [9] and dogs,[10] as was the paucity of elastica material in fatty streak lesions in rabbit aortic lesions.[15] Although endothelium overlying experimental atherosclerotic lesions in the rabbit aorta contained lipid droplets,[15] they rarely did so in human [16] or monkey aorta.[17] A multiple population of cells, consisting of fusiform, stellate and round cells some

of which contained numerous lipid inclusions, was reported in the thickened intima of fatty streak lesions in the human [16] and baboon aorta.[18] The diverse localization within the intima of the round cells filled with lipid droplets and often termed foam cells,[16] has been reported. In rabbit [15] and monkey [17] aortic lesions, foam cells are found lying directly under the endothelium, while in human cerebral arteries they have been reported deeper in the thickened intima.[2] Although round foam cells have been considered to be identical to lipid-filled smooth muscle cells,[15] their derivation from blood monocytes or lymphocytes, as has been frequently suggested,[16,19-21] seems more likely. In this study, smooth muscle cells appear to disintegrate before losing all of their characteristics, and thus form the extracellular debris often found focally. Although intracellular lipid droplets, such as those found in foam cells, have been reported to be crenated after fixation with osmium tetroxide,[16,23] they are found to be round after they are prefixed in glutaraldehyde or paraformaldehyde.[23] Foam-cell lipid droplets, described in human [16,24,25] canine,[19] monkey,[17,18,26] and chicken [27] aortic lesions, have a varied morphology, ranging from vacuoles with empty, partially extracted or electron-dense cores to those filled with homogenous or membranous material and whorl bodies, often together with cholesterol clefts. The empty centers of these vacuoles are believed to be areas in which lipid has been extracted during dehydration and embedding,[16,18,19] while the dissimilarity in structure of the various droplets suggests differences in lipid composition and source. It has been suggested that the vacuoles containing membranous material may be either autophagic [18] or phagocytotic.[16,28] The fact that these vacuoles appear primarily in cells adjacent to extracellular foci of necrosis, filled with such material, strongly suggests that these are phagocytotic vacuoles. In a recent study, however, Wurster and Zilversmit [29] concluded that arterial foam cells derive very little of their extracellular lipid from phagocytosis. If the vacuoles are filled with phagocytosed remnants of necrotic smooth muscle cells, and possibly also plasma lipoproteins, the amorphous droplets may be derived from foam-cell lipid synthesis and plasma lipoproteins previously broken down on the foam cell surface. Numerous foam cells, containing primarily the amorphous type of droplet, have been observed in areas free of smooth muscle cell necrosis, implying that the formation of foam cells from monocytes can occur in the absence of lipid-filled and necrotic smooth muscle cells.

The finger-like extensions of foam cell membranes and their interdigitation have been reported in rabbit [15,30] and monkey [17] lesions and in suspensions of rabbit foam cells,[28] as have the microfibrils, Golgi

zones and smooth endoplasmic reticulum in foam cells of the human aorta [16] and in peritoneal macrophages.[31]

The mononuclear cells with their foot processes, clusters of free ribosomes and pale cytoplasm, but lacking lipid vacuoles, resemble cells seen in human,[16] canine,[19] and baboon [18] aortic fatty streak lesions and human cerebral atheroma.[9] The long strands of rough-surfaced endoplasmic reticulum, sometimes forming a circular array, have been seen in both mononuclear cells [17] and smooth muscle cell pseudopods [26] of monkey aortic lesions. It has been speculated that these mononuclear cells are blood monocytes or lymphocytes that enter the arterial wall,[16] transform into macrophages, engulf extracellular lipid, thereby becoming foam cells, and finally exit from the arterial wall, thus functioning as scavengers.[32] Although cytoplasmic extensions, seen interspersed between foam cells, mononuclear cells and smooth muscle cells, resemble pseudopods of smooth muscle cells seen elsewhere,[33,34] they could also be extensions of mononuclear cells.

The large extracellular accumulations of membranous crystalline material seen in lesions of rabbit,[15] chicken,[27] and human aortic [16,24,25] and cerebral arteries,[9] have been suggested to derive from both cell necrosis and plasma lipoproteins.[18] Such foci of cell necrosis were frequently seen in these fatty streak lesions and are presumed to be the origin of the atheromatous plaque. That these membranous structures are more than cell debris is implied from the fact that areas in which no cells demonstrated signs of necrosis also contained these structures. They may be precipitated plasma lipoproteins which have infiltrated the arterial wall.

The PAS/alcian blue stain on semithick sections of plastic embedded material has been reported for the first time on vascular tissue: It is particularly useful in differentiating smooth muscle from foam cells because of the PAS-positive basement membrane surrounding only the former. The superior resolution obtained by using the technic enables the observer to ascertain structures hereto seen only with the electron microscope. By viewing identical areas with both technics, the identification possibilities afforded by this technic have been substantiated. Procedures are presently being investigated for the use of other stains on plastic-extracted semithick sections.

We concluded, from this study, that the morphology of the fatty streak lesion greatly resembles similar lesions in other arterial beds, both in experimental animals and humans. As was also suggested from the results of histoenzymatic studies on various arterial beds,[12] the documented differences in prevalence of atherosclerosis in intracranial

arteries and the aorta or coronary arteries does not appear to bear either on the structure of each type of lesion or on its progression. Future studies must determine what intrinsic or extrinsic factors cause these differences in the prevalence of atherosclerosis.

References

1. Baker A, Iannone A: Cerebrovascular disease. I. The large arteries of the Circle of Willis. Neurology 9:321–332, 1959
2. Grunnet M: Changes in cerebral arteries with aging. Arch Pathol 88:314–318, 1969
3. Hsieh H: Cerebrovascular disease: a comparative study of cerebral and visceral arteries. Neurology 17:752–762, 1967
4. Lie J, Brown A, Carter: Spectrum of aging changes in temporal arteries. Arch Pathol 90:278–285, 1970
5. Moossy J: Morphology, sites, and epidemiology of cerebral atherosclerosis in cerebral vascular disease, Cerebrovascular Disease, Vol 41. Proceedings of the Association, New York, 1961. Baltimore, The Williams and Wilkins Co, 1966, pp 1–22
6. Stehbens W: Intimal proliferation and spontaneous lipid deposition in the cerebral arteries of sheep and steers. J Atherosclerosis Res 5:556–568, 1965
7. Zugibe F, Brown K: Histochemical studies in atherogenesis: human cerebral arteries. Circ Res 9:897–905, 1961
8. Flora G, Dahl E, Nelson E: Electron microscopic observations on human intracranial arteries: changes seen with aging and atherosclerosis Arch Neurol 17:162–173, 1967
9. Imai H, Thomas W: Cerebral atherosclerosis in swine: role of necrosis in progression of diet-induced lesions from proliferative to atheromatous stage. Exp Mol Pathol 8:330–357, 1968
10. Suzuki M: Experimental cerebral atherosclerosis in the dog. I. A morphologic study. Am J Pathol 67:387–402, 1972
11. Martinez A: Electron microscopy of human atherosclerotic cerebral vessels. Int Congress Neuropathol 2, 164–169, 1972
12. Hoff HF: A histoenzymatic study of human intracranial atherosclerosis. Am J Pathol 67:263–280, 1972
13. Solberg L, Eggen D: Localization and sequence of development of atherosclerotic lesions in the carotid and vertebral arteries. Circulation 430:711–724, 1971
14. Mayor H, Hampton J, Rosario B: A simple method for removing the resin from epoxy-embedded tissue. J Biophys Biochem Cytol 9:909–910, 1961
15. Parker F, Odland G: A correlative histochemical, biochemical and electron microscopic study of experimental atherosclerosis in the rabbit aorta with special reference to the myo-intimal cell. Am J Pathol 48:197–239, 1966
16. Geer J: Fine structure of human aortic intimal thickening and fatty streaks. Lab Invest 14:1764–1783, 1965
17. Tucker C, Catsulis C, Strong J, Eggen D: Regression of early cholesterol-induced aortic lesions in rhesus monkeys. Am J Pathol 65:493–514, 1971
18. Geer J, Catsulis C, Mcgill H, Strong J: Fine structure of the baboon aortic fatty streak. Am J. Pathol 52:265–286, 1968

19. Geer J: Fine structure of canine experimental atherosclerosis. Lab Invest 47:241–269, 1965
20. Suzuki M: Experimental atherosclerosis in the dog: a morphologic study. Exp Mol Pathol 3:455–467, 1964
21. Still W, Dennison S: Reaction of the arterial intima of the rabbit to trauma and hyperlipemia. Exp Mol Pathol 6:245–253, 1967
22. Haust M: The morphogenesis and fate of potential and early atherosclerotic lesions in man. Hum Pathol 2:1–29, 1971
23. Hoff HF: Studies on the pathogenesis of atherosclerosis with experimental model systems. IV. Ultrastructural and lipid-histochemical changes in the lipoprotein-filled doubly ligated carotid artery. Virchows Arch A(Pathol) 352:99–110, 1971
24. Ghidoni J, O'Neal R: Recent advances in molecular pathology, a review: ultrastructure of human atheroma. Exp Mol Pathol 7:378–400, 1967
25. Balis J, Haust M, More R: Electron microscopic studies of human atherosclerosis: cellular elements in aortic fatty streaks. Exp Mol Pathol 3:511–525, 1964
26. Scott R, Jones R, Daoud A, Zumbo O, Carlston F, Thomas W: Experimental atherosclerosis in rhesus monkeys. II. Cellular elements of proliferative lesions and possible role of cytoplasmic degeneration in pathogenesis as studied by electron microscopy. Exp Mol Pathol 7:34–57, 1967
27. Moss N, Benditt E: The ultrastructure of spontaneous and experimentally induced arterial lesions III. The cholesterol-induced lesions and the effect of a cholesterol and oil diet on the pre-existing spontaneous plaque in the chicken aorta. Lab Invest 23:521–535, 1970
28. Newman H, Murad T, Geer J: Foam cells of rabbit atheromatous lesion: identification and cholesterol uptake in isolated cells. Lab Invest 25:586–595, 1971
29. Wurster N, Zilversmit D: The role of phagocytosis in the development of atherosclerotic lesions in the rabbit. Atherosclerosis 14:309–322, 1971
30. Peterson M, Day A, Tume R, Eisenberg E: Ultrastructure, fatty acid content and metabolic activity of foam cells and other fractions separated from rabbit atherosclerotic lesions: Exp Mol Pathol 15:157–169, 1971
31. Nichols B, Bainston D, Farquhar M: Differentiation of monocytes: origin, nature, and fate of their azurophil granules. J Cell Biol 50:498–515, 1971
32. Day A: The macrophage system: lipid metabolism and atherosclerosis J Atherosclerosis Res 4:117–130, 1964
33. Hoff HF, Gottlob R: Ultrastructural changes of large blood vessels following mild mechanical trauma. Virchows Arch A(Pathol) 345:93–106, 1968
34. Hoff HF, McDonald L, Hayes T: An electron microscope study of the rabbit aortic intima after occlusion by brief exposure to a single ligature. Br J Exp Pathol 49:68–73, 1968
35. Moss N, Benditt E: The ultrastructure of spontaneous and experimentally induced arterial lesions II. The spontaneous plaque in the chicken. Lab Invest 23:231–245, 1970
36. Haust M, Geer J: Mechanism of calcification in spontaneous aortic arteriosclerotic lesions of the rabbit: an electron microscopic study. Am J Pathol 60:329–346, 1970

Legends for Figures

Fig 1—PAS–alcian blue stain of 0.5μ-thick sections of Epon-embedded intracranial arteries. Sections photographed with a green filter to accentuate red PAS-positive material; *l* = lumen; *a–e* = intimal surface; all micrographs (× 650). **A**—Note PAS-positive material subjacent to endothelium, around fusiformed smooth muscle cells, but not circumscribing foam cells (fo) grouped close together near lumen. **B**—Numerous smooth muscle cells with PAS-positive basement membranes, some containing lipid droplets (*arrows*) are seen subjacent to the lumen. Groups of foam cells deeper in thickened intima. Note PAS-positive granules in some foam cells. **C** and **D**—Foam cell clusters below several layers of smooth muscle cells. Note how lipid droplets comprise entire cytoplasm of foam cells in contrast to smooth muscle cell. **E**—Foam cells dispersed throughout this part of thickened intima. Note basement membrane missing around some parts of smooth muscle cells (*arrows*). Although lipid droplets in foam cells are usually of uniform size, numerous large droplets can be seen together with smaller ones. **F**—Some oval or round cells (*arrows*) subjacent to endothelium without a basement membrane or lipid droplets. **G**—Note thicker and more intense PAS-positive staining of basement membrane around medial smooth muscle cells (lower part of micrograph) than around those in intima (*el* = elastica). **H**—Numerous lipid droplets of different sizes in intimal smooth muscle cells.

Fig 2—PAS–alcian stain of 0.5μ–thick sections of Epon-embedded intracranial arteries, *l* = lumen; *a–g* = intimal surface; *h* = deeper intima, all micrographs (× 650). **A**—Area of thickened intima which is relatively narrow. Hardly any foam cells are seen and lipid droplets are primarily in smooth muscle cells, *el* = elastica. **B**—As in **A**, a thick band of PAS-positive material is subjacent to endothelium. Below this band are some foam cells; numerous smooth muscle cells contain lipid droplets, *el* = elastica. **C**—Line of foam cells deeper in thickened intima. Note smooth muscle cell (*arrow*) in which lipid droplets fill entire upper part of cytoplasm while few droplets are in the lower part. Basement membrane does not completely circumscribe this cell. **D**—This area of thickened intima can be termed a foam-cell lesion, since almost the entire area is packed with such cells lying just underneath the thin endothelium. Note PAS-positive material between these cells and in intracellular granules. Some smaller cells are devoid of lipid droplets. **E**—Another foam-cell lesion in which some cells, devoid of lipid, can be seen subjacent to endothelium, as can narrow bands of smooth muscle cells, identified by their PAS-positive basement membrane. Notice some cells partially filled with lipid and circumscribed by incomplete basement membrane (*arrows*). **F**—Foam cells interspersed between smooth muscle cells. Dark area below endothelium was PAS-positive. **G**—Foam cells grouped together deeper in thickened intima. Note PAS-positive granules and narrow smooth muscle cells which only infrequently contained lipid droplets. **H**—Smooth muscle cells (*sm*) can be seen between foam cells (*fo*) and mononuclear cells (*mo*) devoid of lipid.

Fig 3—Low power electron micrographs of fatty streak lesions in intracranial arteries, *l* = lumen. **A**—Thickened intima filled primarily with smooth muscle cells (sm), some containing lipid droplets (li) without a limiting membrane. The endothelial lining is patent and resembles that in uninvolved areas. A fragmented basement membrane surrounds each smooth muscle cell. Even the cell filled with lipid droplets, crystalline material and whorl bodies appears to have some basement membrane around part of its surface (× 6,700). **B**—Center of a foam cell lesion. Note close packed arrangement of most cells, some containing vacuoles filled with membranous material (*mb*) or lipid droplets (*li*), usually with a limiting membrane; other cells (*mo*) are devoid of lipid droplets. Extracellular space (es) also filled with membranous material (× 8,000).

Fig 4A—Intimal surface of a fatty streak lesion, *l* = lumen. Notice the extracellular area below the endothelium and between the smooth muscle cells (*sm*). Found between the granular basement membrane of the smooth muscle cells are round electron-translucent areas (*x*) of various sizes with poorly outlined limiting membranes of different electron densities. Smooth muscle cell on *left* has usual myofibrils, rough endoplasmic reticulum, mitochondria and cell membrane invaginations. Note perinuclear localization of lipid droplet (*li*) devoid of limiting membrane. Cell on right, filled with lipid vacuoles, believed to be smooth muscle cell even though it is circumscribed by very little basement membrane (× 7,600). **B and C**— Note round and reticulated electron-translucent material (*x*) between smooth muscle cells (**B,** × 13,600; **C,** × 14,500).

Fig 5A—This micrograph demonstrates the extensive interdigitation of foot processes between foam cells. Very little extracellular space is found in such groups of foam cells (× 15,300). **B**—At higher magnification the morphology of two foam cells, this time separated by a straight junction, can be clearly seen. Besides rough and smooth endoplasmic reticulum, swollen mitochondria, electron-dense and PAS-positive bodies (*arrows*), microtubules (*mt*) and filaments (*f*), one can see lipid vacuoles (*li*) and crystalline material suggested to be a cholesterol ester cleft; (*cl*) (× 32,000).

Fig 6A—Although granular, PAS-positive material is found between such cells, as depicted in this micrograph, the morphology is typical for a foam cell (Figure 5B) (× 33,000). **B**—On numerous occasions such dense bodies comprised of a whorl body and a crystalline cleft, can be found in foam cells and occasionally in smooth muscle cells (× 34,000). **C**—A common type of lipid droplet in foam cells is one in which the electron-dense contents are partially extracted. Round arrays close to the cell border (*arrow*) are presumed to be foot processes from either this or another foam cell. On the upper part of the micrograph is part of a mononuclear cell (*mo*) devoid of lipid (× 24,000).

Fig 7A—Foam cells adjacent to extracellular space (es) which is filled with membranous material, usually contain numerous vacuoles filled with such membranous material (*arrow*) (× 20,000). **B**—At a junction of numerous cells including a mononuclear cell with long rough surfaced endoplasmic reticulum (*arrow*), one can also see an arm or pseudopod of another cell (*x*) either derived from a mononuclear or smooth muscle cell (× 19,700).

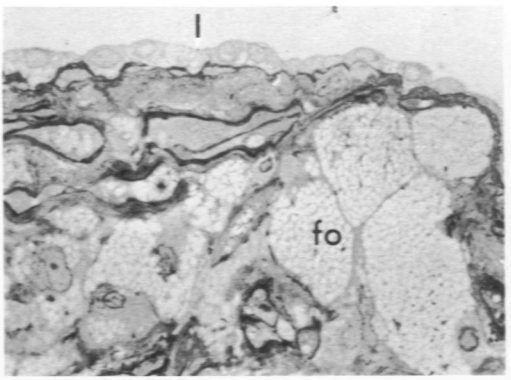

1A

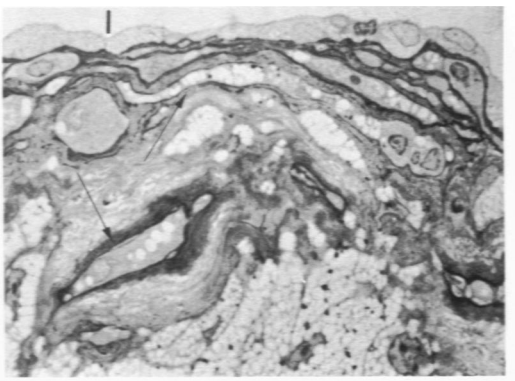

1B

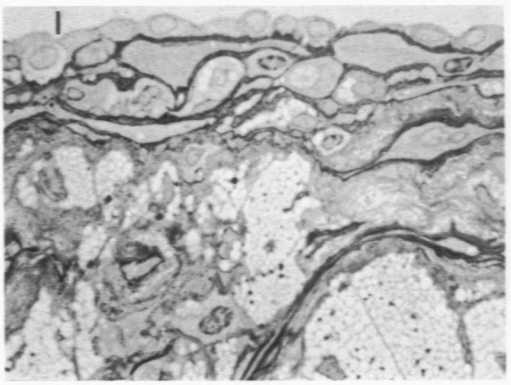

1C

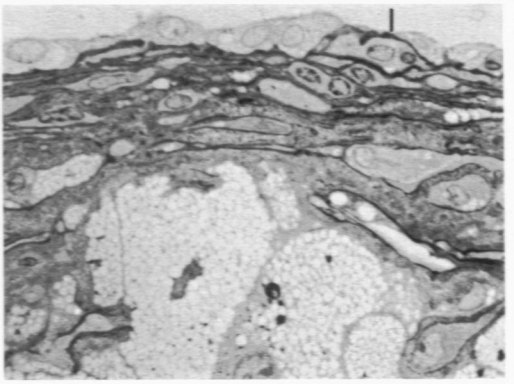

1D

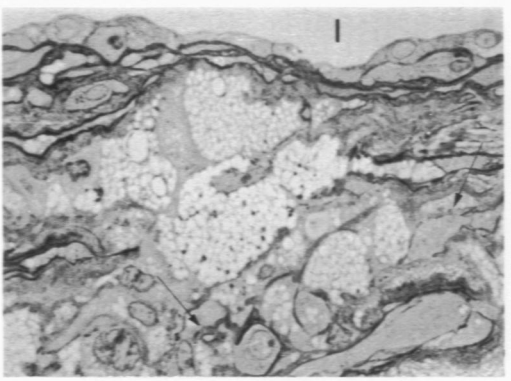

1E

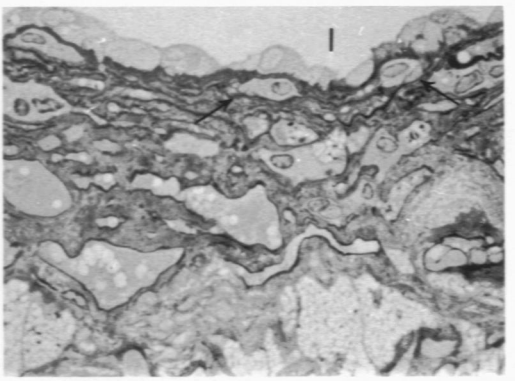

1F

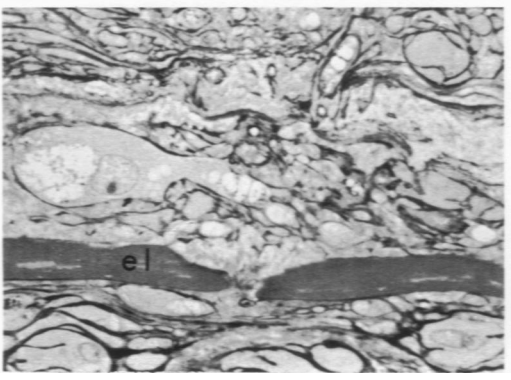

1G

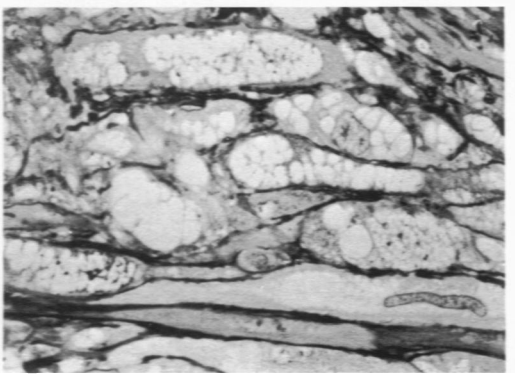

1H

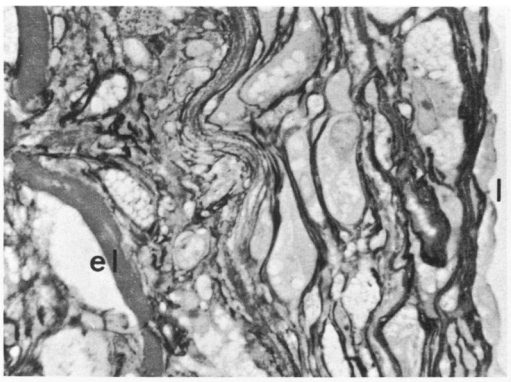

2A

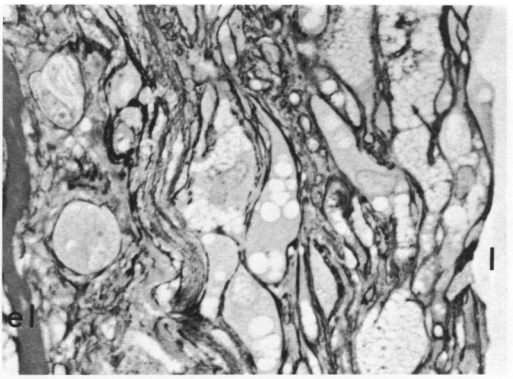

2B

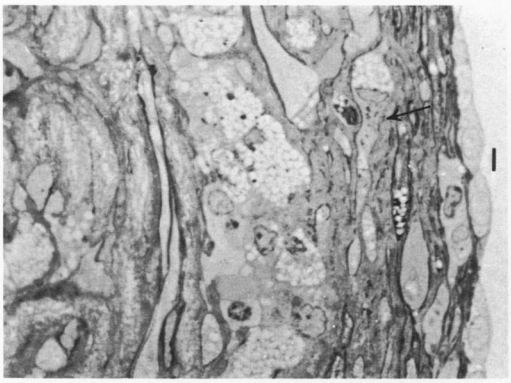

2C

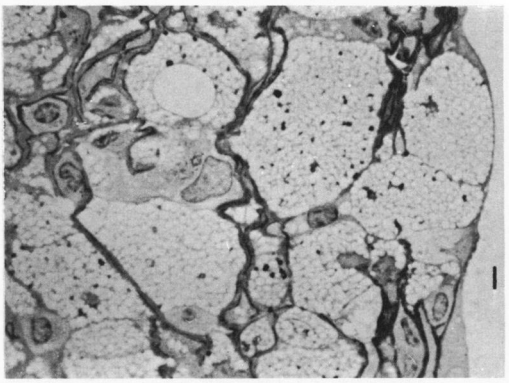

2D

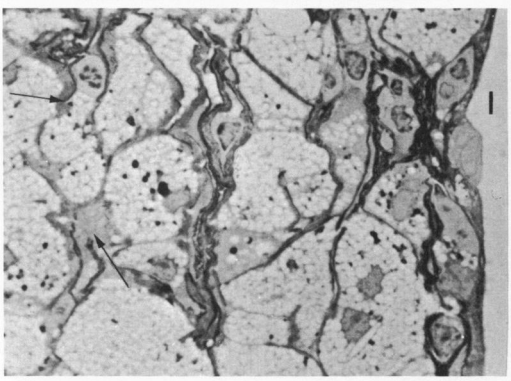

2E

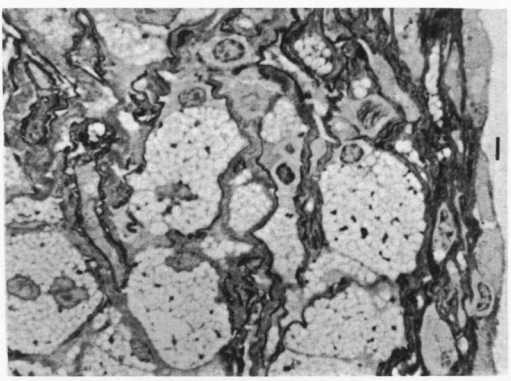

2F

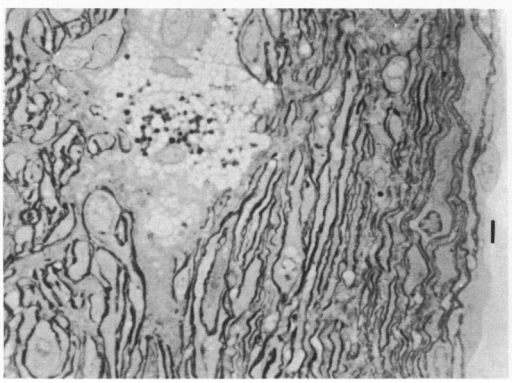

2G

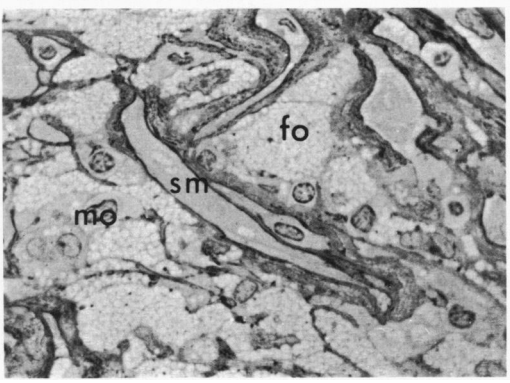

2H

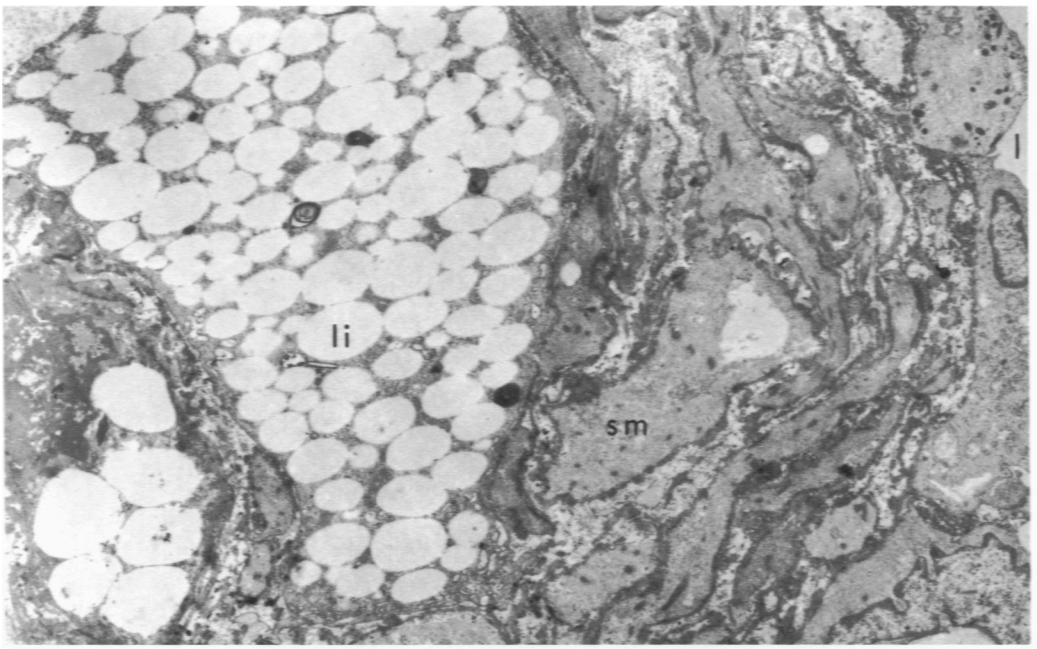

3A

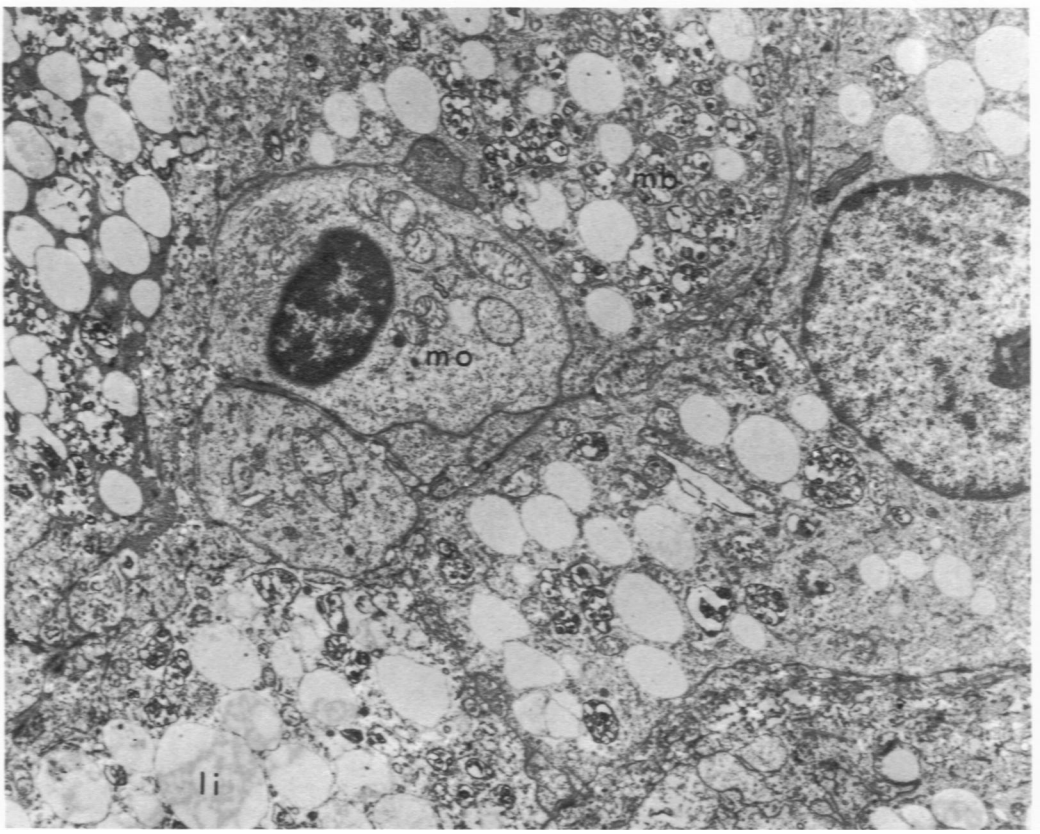

3B

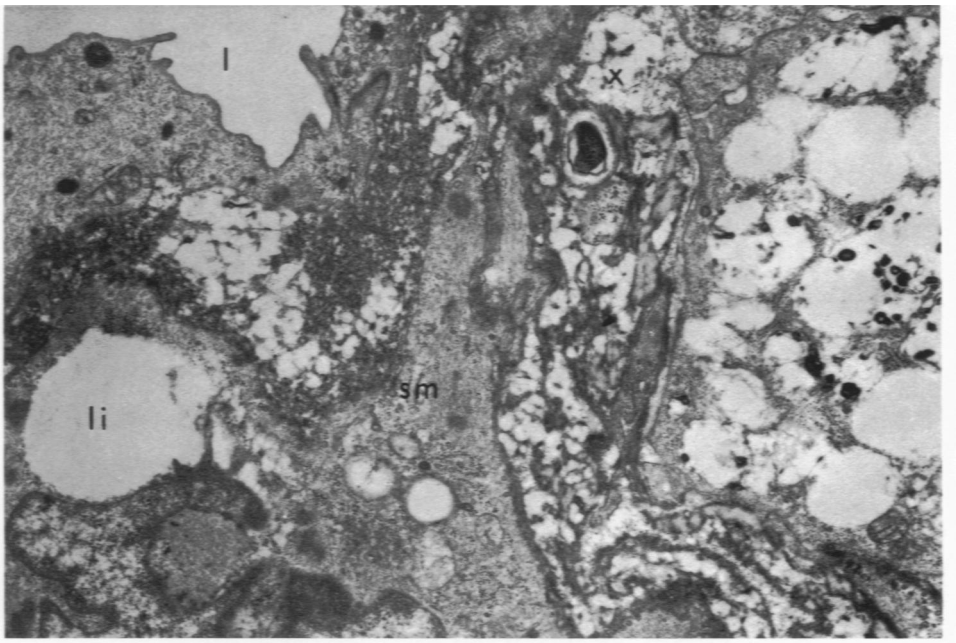

4A

4B

4C

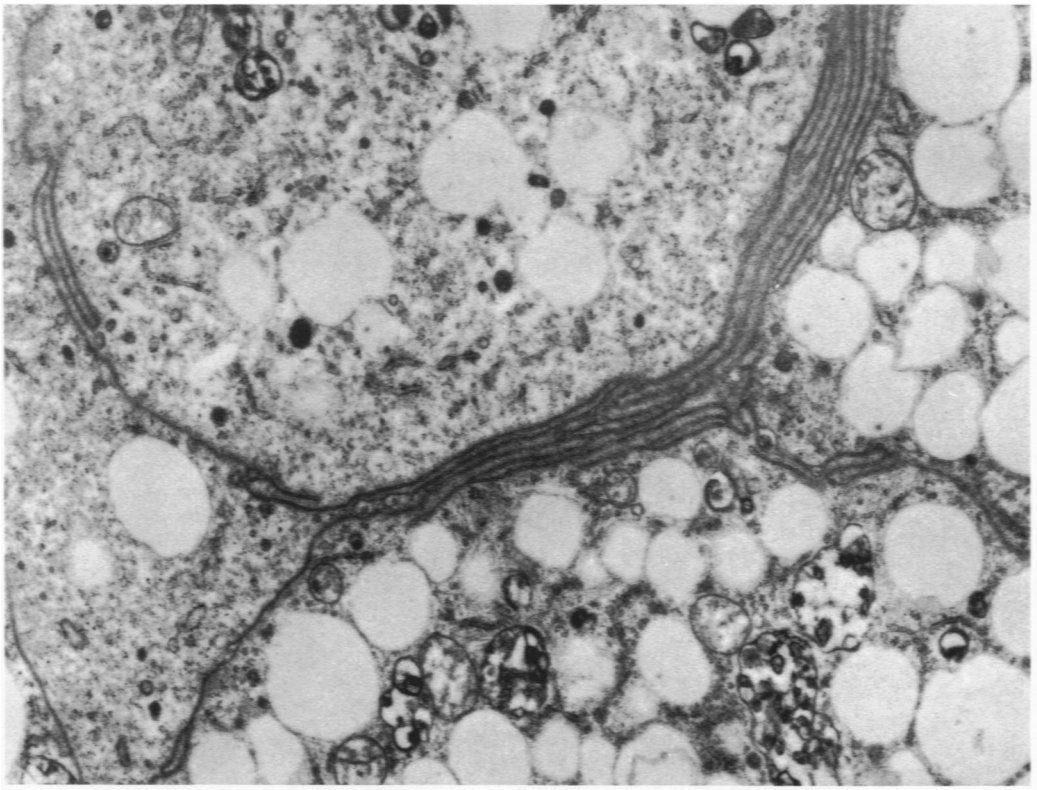

5A

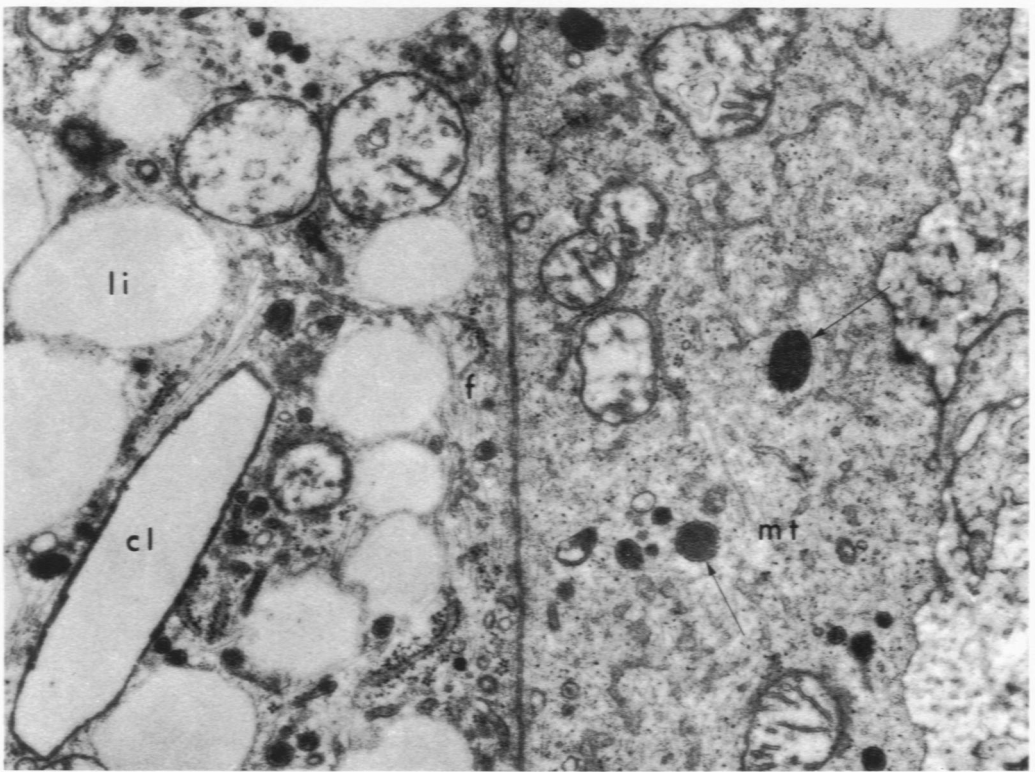

5B

6A

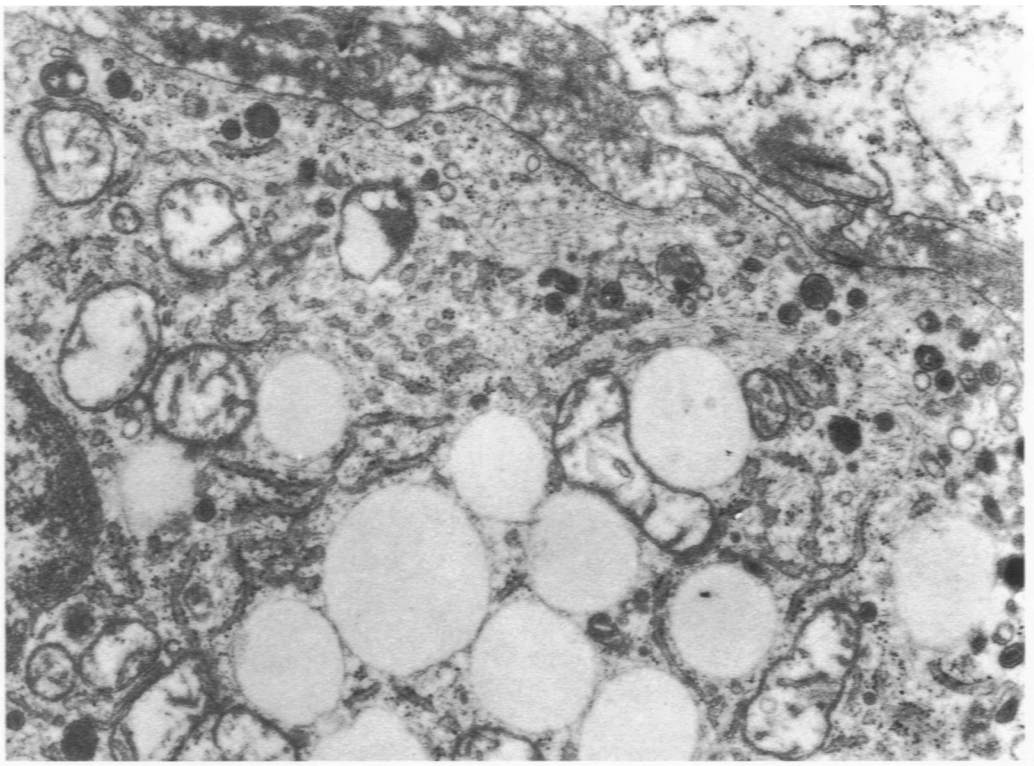

6B

6C

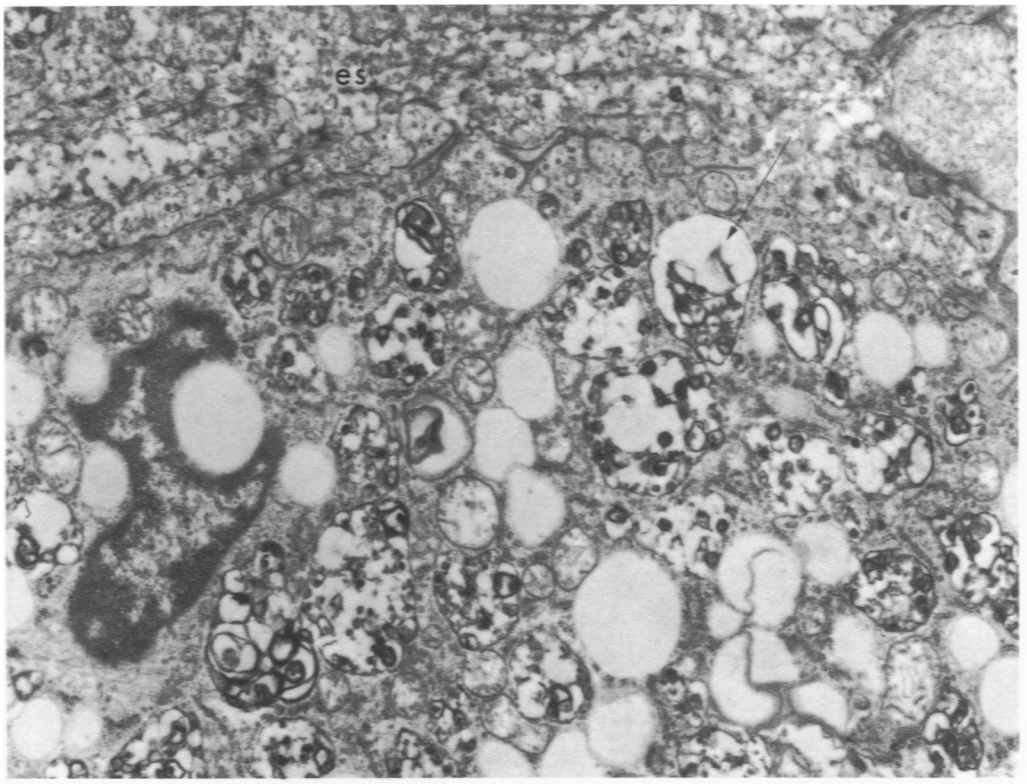

7A

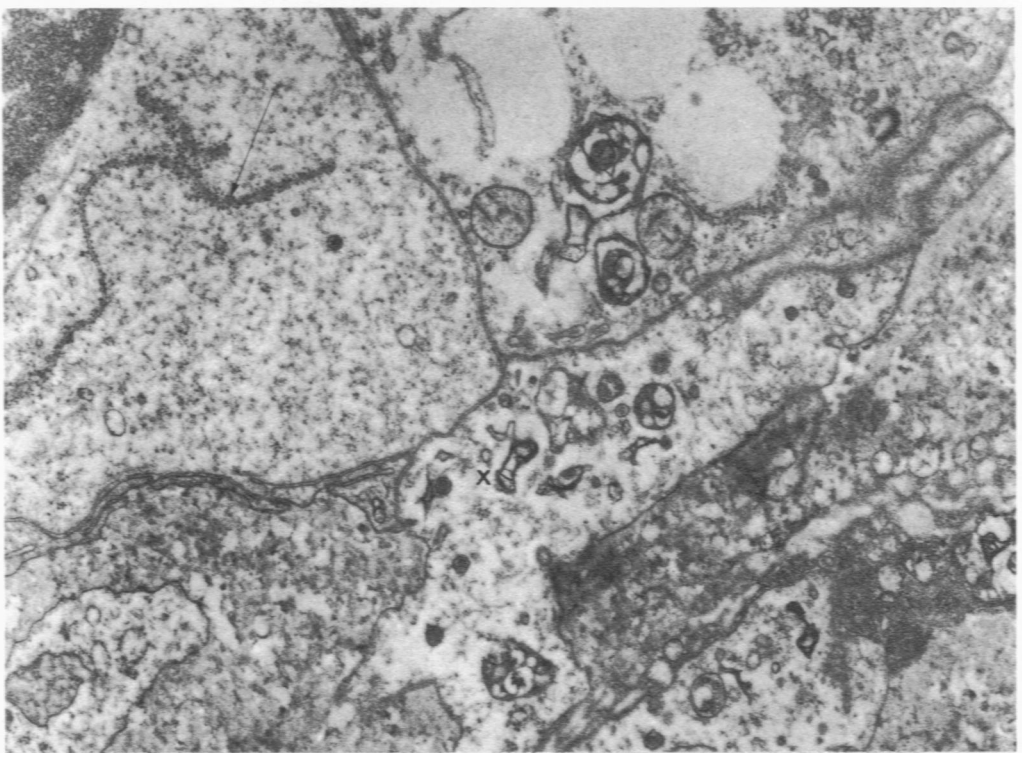

7B

[*End of Article*]